


# Antibacterial effect of bismuth subsalicylate nanoparticles synthesized by laser ablation

Mariela Flores-Castañeda · Alejandro L. Vega-Jiménez  · Argelia Almaguer-Flores · Enrique Camps · Mario Pérez · Phaedra Silva-Bermudez · Edgardo Bera · Sandra E. Rodil

Received: 25 June 2015 / Accepted: 24 October 2015 / Published online: 3 November 2015  
© Springer Science+Business Media Dordrecht 2015

**Abstract** The antimicrobial properties of bismuth subsalicylate (BSS) nanoparticles against four opportunistic pathogens; *E. coli*, *P. aeruginosa*, *S. aureus*, and *S. epidermidis* were determined. BSS nanoparticles were synthesized by pulse laser ablation of a solid target in distilled water under different conditions. The nanoparticles were characterized using high-resolution transmission electron microscopy and absorption spectra and small angle X-ray scattering. The analysis shows that the colloids maintained the BSS structure and presented average particle size between 20 and 60 nm, while the concentration ranges from 95 to 195 mg/L. The antibacterial effect was reported as the inhibition ratio of the bacterial growth after 24 h and the cell viability was measured using the XTT assay.

The results showed that the inhibition ratio of *E. coli* and *S. epidermidis* was dependant on the NPs size and/or concentration, meanwhile *P. aeruginosa* and *S. aureus* were more sensitive to the BSS nanoparticles independently of both the size and the concentration. In general, the BSS colloids with average particle size of 20 nm were the most effective, attaining inhibition ratios >80 %, similar or larger than those obtained with the antibiotic used as control. The results suggest that the BSS colloids could be used as effective antibacterial agents with potential applications in the medical area.

**Keywords** Bismuth subsalicylate · Nanoparticles · Laser ablation · Antimicrobial effect · Health effects

---

M. Flores-Castañeda · E. Camps · M. Pérez  
Instituto Nacional de Investigaciones Nucleares,  
Apdo. Postal 18-1027, CP 11801 Mexico, D. F., Mexico

A. L. Vega-Jiménez (✉) · A. Almaguer-Flores  
Facultad de Odontología, DEPeI, I, Universidad Nacional  
Autónoma de México, Circuito exterior s/n, Ciudad  
Universitaria, CP 04510 Mexico, D. F., Mexico  
e-mail: argelia.almaguer@mac.com

P. Silva-Bermudez  
Unidad de Ingeniería de Tejidos, Terapia Celular y  
Medicina Regenerativa, Instituto Nacional de  
Rehabilitación, Calz. México-Xochimilco No. 289, Col.  
Arenal de Guadalupe, CP 14389 Mexico, D. F., Mexico

E. Bera  
FarmaQuimía SA de CV., Ampere No. 11, Parque  
Industrial Cuamatla, CP 54730 Cuautitlan Izcalli,  
Estado de México, Mexico

S. E. Rodil  
Instituto de Investigaciones en Materiales, Universidad  
Nacional Autónoma de México, Circuito exterior s/n,  
Ciudad Universitaria, CP 04510 Mexico, D. F., Mexico

## Introduction

Different based-bismuth compounds have been used in medicine for the treatment of a variety of gastrointestinal disorders related with the presence of *Helicobacter pylori* (Delchier et al. 2014; Ge et al. 2012; Pacifico et al. 2012; Tillman et al. 1996). In addition, numerous studies have reported the use of bismuth salts as components of haemostatic wound dressings (Kim et al. 2012; Tramontina et al. 2002), local antiseptics (Serena et al. 2007) and biocompatible radiopaque agents (Hernandez et al. 2007; Kim et al. 2008). Based on the well-known sensitivity of *H. pylori* to bismuth compounds like bismuth subsalicylate (BSS), bismuth subnitrate (BSN), and colloidal bismuth subcitrate (BSC), the antibacterial effect of these compounds against other microorganisms such as *Clostridium difficile* (Mahony et al. 2005), *Pseudomonas aeruginosa* (Alipour et al. 2011), *Escherichia coli* (Brogan et al. 2005), and *Staphylococcus* sp. (Shaikh et al. 2007) among others, had also been studied.

The first reports concerning the therapeutic uses of bismuth subsalicylate included the treatment of early syphilis (Pardo and Pardo Castello 1952), diarrhea (DuPont 1987; DuPont et al. 1977), and even viral gastroenteritis (Steinhoff et al. 1980). In the same fashion, there are numerous studies regarding the effectiveness of this compound in the inhibition of the growth of species related to gastrointestinal disorders like *Escherichia coli*, *Salmonella*, *Shigella* and *Campylobacter* sp. (Andreasen and Andersen 1987; Cornick et al. 1990; Manhart 1990). It is important to mention that the antibacterial activity of BSS is attributed to the water-soluble bismuth products produced by the interaction of insoluble bismuth compounds with dietary components and organic substrates (Mahony et al. 2005). It has been proposed that the crystalline structure of bismuth subsalicylate and the bismuth oxide cores of this compound control its antimicrobial activity (Andrews et al. 2006; Manhart 1990). The reports regarding the mechanism of action of BSS suggest that this compound can inactivate Gram negative toxins (Ericsson et al. 1977), additionally, bacteria exposed to BSS may have a cessation of ATP synthesis and a loss of membrane integrity causing their inhibition growth (Sox and Olson 1989).

In recent years, the use of nanoparticles has been proposed as possible new antimicrobial agents (Botequim et al. 2012; Hajipour et al. 2012; Huh and Kwon

2011). Many studies suggested that nanoparticles with antibacterial effects could be less toxic to eukaryotic cells and more important, could reduce microbial resistance compared to conventional antibiotics (Goodman et al. 2004; Schaller et al. 2004; Weir et al. 2008).

Regarding the potential uses of bismuth nanoparticles in the medical field for antimicrobial activity, few reports, in comparison to those concerning Ag or Cu NPs, have been published (Hernandez-Delgadillo et al. 2012, 2013; Nazari et al. 2014) and such papers are related to metallic bismuth nanoparticles. The aim of the present work was to evaluate the antimicrobial activity of bismuth subsalicylate nanoparticles (BSS-NPs), in order to demonstrate their possible applications as antibacterial agent in a colloidal presentation, similar to the well-known colloidal silver solutions (dos Santos et al. 2014; Markowska et al. 2013; Mijndonckx et al. 2013).

The first challenge was the production of the BSS nanoparticles, for which pulsed laser ablation (PLA) of a BSS target in water was chosen as the most suitable technique. Immersed PLA is known as a physical vapor deposition technique that allows the formation of NPs keeping the composition and chemical structure of the target material (Yang 2012). Due to the low solubility of the BSS on water, it was possible to obtain BSS in a colloidal presentation. In this study, the antibacterial activity was evaluated against four opportunistic pathogens, two Gram negative species; *E. coli* and *P. aeruginosa* that have been reported as the first causes of chronic wound and orthopedic-implant infections (Cremet et al. 2015; Rybtke et al. 2015). Additionally, two Gram positive strains *Staphylococcus aureus* and *Staphylococcus epidermidis* were also included in the study; these species are responsible for the biofilm growth found on explanted orthopedic devices and in recent years have emerged as some of the most important causes of nosocomial infections (Harris et al. 2002; Riool et al. 2014).

## Materials and methods

### Synthesis and characterization of the BSS nanoparticles

The BSS-NPs were produced using the laser ablation of solids immersed in water, using the experimental

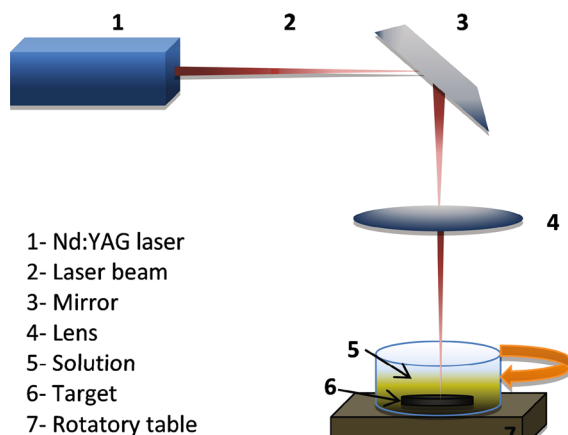


**Fig. 1** Schematic of the experimental setup used for the synthesis of the BSS nanoparticles using pulsed laser ablation of solids in liquids

setup shown in Fig. 1. A Nd: YAG laser emitting at the fundamental wavelength of 1064 nm, with a 28 ns pulse duration, a repetition rate of 20 Hz and a maximum output energy of 135 mJ was used. The bismuth subsalicylate ( $C_7H_5BiO_4$ ) target 99.99 % purity (FQ specialties SA de CV) was placed at the bottom of the glass and immersed in distilled water. The laser was directed to the target surface using a mirror and a focusing lens. During the ablation process, the glass container was rotated in order to avoid drilling of the target. Synthesis parameters like the ablation time and lens distance were manipulated to modify two important characteristics of NPs: the average size and the concentration. The nanoparticle average size was varied by changing the energy density deposited on the target surface; such energy variation was achieved by adjusting the focusing lens distance, while the nanoparticles concentration was

changed by adjusting the ablation time (Table 1). The name of the sample was given depending of the average size obtained in each sample, i.e., BSS-60 (58 nm), BSS-45 (45 nm), BSS-30 (31 nm) and 20 (22 nm).

Transmission electron microscopy (TEM) measurements were performed using a JEOL JEM 2010 at an acceleration voltage of 200 kV. Energy dispersive spectroscopy (EDS) measurements were also carried out in the TEM.

The particle size distributions obtained by TEM correspond only to the counting of a reduced number of NPs, thus to obtain a more representative average particle size, small angle X-ray scattering (SAXS) measurements were performed. The SAXS measurements were performed using an Ultima IV X-ray Rigaku diffractometer in the transmission mode of the small angle scattering stage. The SAXS patterns, scattering intensity versus  $2\theta$ , are produced due to the differences in the electron density between the particles and the surrounding media, so it depends on the form of the particles. Therefore, for the simulation of the SAXS profiles, BSS spherical particles in water were assumed. The simulation was performed using the Rigaku-Nanosolver program leading to the average diameter and variance. The advantage of the SAXS method is that it measures the colloids placed directly into glass capillaries without further preparation, so it is a nondestructive and quick method.

To determine the concentration of the BSS in the colloids, five samples were prepared at fixed lens distance (22 cm) and laser power (130 mJ), while the ablation time was increased from 2 to 7 min. The UV–Vis absorption at 280–295 nm was correlated to the corresponding mass-weight of the samples prepared at

**Table 1** Synthesis parameters and characteristics of the BSS colloidal samples

Samples	Lensdistance (cm)	Ablationtime (min)	Concentration (mg/L) <sup>a</sup>	Size (nm) <sup>b</sup>	Dispersion (%) <sup>c</sup>
BSS-60	21	4	183	58	60
BSS-45	22	4	150	45	72
BSS-30	23	4	95	31	69
BSS-20	24	8	193	22	84

<sup>a</sup> Concentration determined using the calibration curve shown in Fig. 5

<sup>b</sup> Average size measured using SAXS (Fig. 3)

<sup>c</sup> Dispersion of the average size obtained from the SAXS analysis (Fig. 3)

different ablation times using the Beer-Lambert law. The mass-weight of each sample was obtained after evaporating the water at 80 °C for 5 h. Using these five data, an extended calibration curve was constructed where the mass-weight of these five samples was plotted versus the maximum of the absorption band. This calibration curve allows us to estimate the concentration of any other sample just by measuring the maximum absorption in the 280–290 nm range. In addition, due to the fact that the UV–Vis spectra are quite sensitive to any change in the studied colloid, the stability in time of the colloids was also evaluated using the UV–Vis spectra.

#### Antibacterial assays

The bacterial strains used in this study were *E. coli* (ATCC 33780), *P. aeruginosa* (ATCC 43636), *S. aureus* (ATCC 25923) and *S. epidermidis* (ATCC 14990). All the strains were obtained as freeze-dried cultures of American Type Culture Collection (ATCC). For the experiments, the growth of pure cultures of each strain was harvested from agar surfaces and suspended in individual tubes with enriched TSB (Trypticase soy broth) added with 0.3 µg/mL menadione (Sigma-Aldrich) and 5 µg/mL hemin (Sigma-Aldrich). The optical density (OD) of each tube was adjusted in a spectrophotometer at 600 nm, in order to obtain 10<sup>9</sup> bacterial cells per milliliter of each strain. Then, 20 µL of the adjusted suspension of the four bacterial strains were individually transferred in 96-well microplates and the four different samples of BSS-NPs were tested against each strain in a total volume of 200 µL. Culture medium was used as negative control and Ciprofloxacin (180 µg/mL) was used as positive control. The bacterial strains with the BSS-NPs were incubated at 37 °C using orbital shaking at 160 rpm during 24 h. After the incubation, cell viability was analyzed using the XTT-PMS assay (Sigma-Aldrich); 10 µL of XTT-PMS reagent was added to each well and incubated during 3 h at 37 °C, then the absorbance was measured at 450 nm (reference wavelength 620 nm) using the FilterMax F5 (Molecular Devices, USA). All tests were run in triplicate.

The antibacterial effectiveness of the BSS-NPs was expressed as the inhibition ratio according with the following equation:

$$\text{Inhibition Ratio (\%)} = \left( \frac{A1 - A2}{A1} \right) \times 100$$

where, A1 Absorbance at 450 nm in for the bacteria in the culture medium (negative control), A2 Absorbance at 450 nm in presence of a bacterial growth inhibitor; Antibiotic (positive control) or BSS-NPs.

Additionally, bacterial growth curves were made in order to determine if the inhibitory effect was either bactericidal (killing effect) or bacteriostatic (growth inhibition). The four bacterial strains adjusted to 10<sup>9</sup> mL were individually placed in 96-well microplates with or without BSS NPs in a total volume of 200 µL. The bacterial strains were incubated at 37 °C using orbital shaking at 160 rpm and the absorbance was measured at 620 nm using the FilterMax F5 at 4, 8, 12, 24, 48, and 72 h.

The data analysis for the antibacterial tests was performed using ANOVA, and significant differences between the samples were determined using Bonferroni's modification.

## Results

### Characterization of the BSS Nanoparticles

#### Size distribution

**Transmission electron microscopy, TEM** Transmission electron microscopy was done on the colloids synthesized at different ablation conditions, obtaining spherical nanoparticles (NPs) in a wide range of particle size. The results suggested that the focusing distance was the main parameter controlling the average size of the BSS-NPs.

One example (focusing lens distance of 24 cm) of the high-resolution TEM images is shown in Fig. 2a, b. The images were used to measure the interplanar space of the observed crystalline nanoparticles. The interplanar distances were 3.67, 9.85, and 4.91 Å corresponding to the (302), (011), and (22-1) planes for the BSS structure, respectively, as reported in the PDF cards (7001563 and 7001555). Moreover, a EDS analysis was performed and the spectra (not shown) confirmed the presence of bismuth and oxygen in a 1:4 compositional ratio, as in the BSS (C<sub>7</sub>H<sub>5</sub>BiO<sub>4</sub>) without other elements.

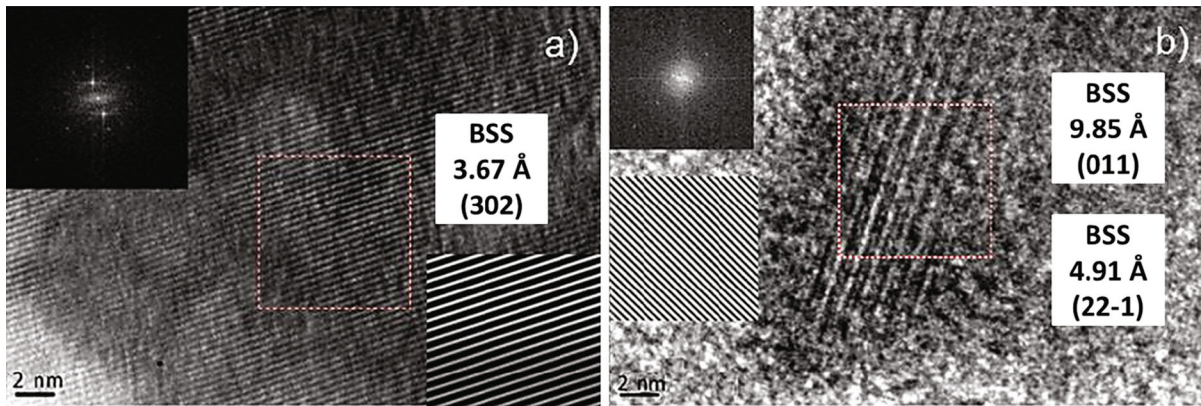


**Fig. 2** a, b High-resolution TEM images of the BSS nanoparticles. The inset shows the electron diffraction pattern image of SSB nanoparticles

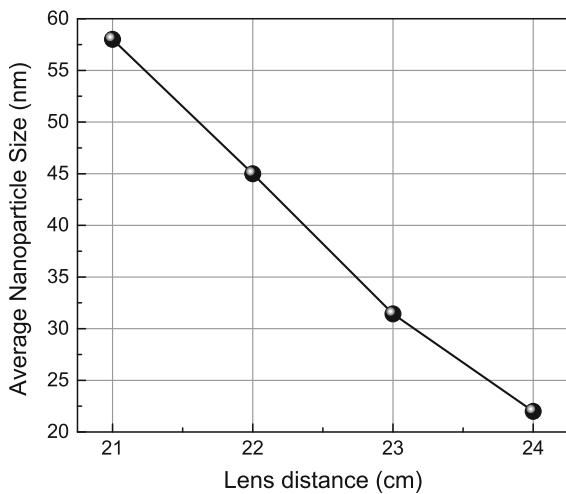


**Fig. 3** Small angle X-ray scattering profiles for the colloids synthesized at different lens distances, but keeping the ablation time and laser power fixed. The normalized distribution was obtained assuming spherical nanoparticles

*Small angle X-ray scattering, SAXS* Since sample preparation and analyses using HRTEM were time consuming and not necessarily representative of the average size of the NPs produced under each one of the synthesis conditions, then a set of samples produced at different focusing lens distances were produced for SAXS analysis. Figure 3 shows the variation of the average size as a function of the lens distance, the overall behavior observed was that the larger the lens distance, the lower the nanoparticle size. Such a result was expected since as the focusing lens is separated from the target, the area (or spot size) where the laser

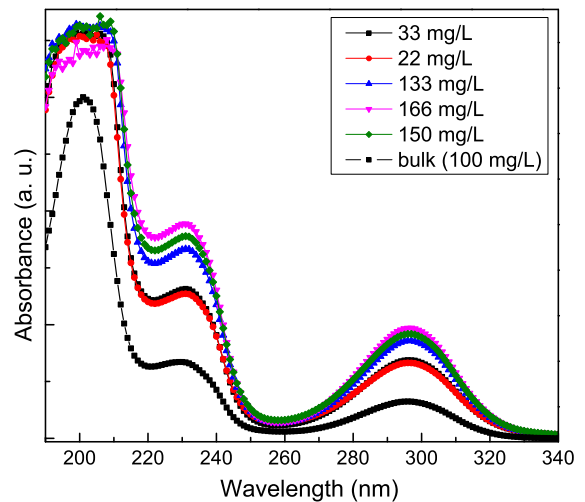


**Fig. 4** UV-Vis absorption spectra of BSS nanoparticles in aqueous solution

deposits its energy increases, and then the density of energy deposited on the target decreases (Yang 2012). The information presented in Table 1 included the average diameter and the size dispersion of the BSS NPs from the analysis of the SAXS profiles.

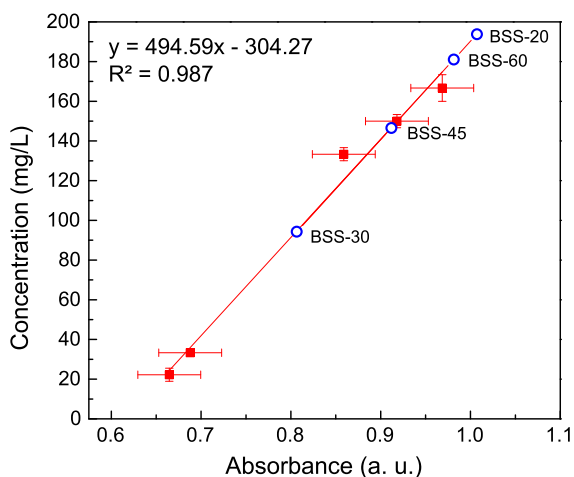
*Concentration and stability*

Figure 4 shows the absorption spectra of the colloids reported in Table 1 and the spectrum of 100 mg/L of BSS-salt in water is also shown. Although, we could not find molecular reference spectra that allow the proper identification of BSS, the fact that similar



absorption bands are observed for the dispersed salt in water and the colloidal solution obtained after the ablation process is a good indication of a similar molecular structure. The BSS is considered as a bismuth oxide core structure with salicylate ions attached to the surface or as a bismuth salt of salicylic acid; therefore, the functional groups associated to the salicylic acid are expected to dominate the UV–Vis spectra. The UV–Vis spectrum of dissolved salicylic acid shows two main electronic absorption bands about 234–237 and 296–303 nm depending on the medium (Purvis 1926, 1927), being the latter the most intense and characteristic. Both peaks are in good agreement with the two signals observed in Fig. 4, suggesting that indeed the UV–Vis spectra are dominated by the electronic transitions from the salicylic molecule (the lower band around 190 nm is not very precise since the cut-off wavelength for water is about 205 nm). Moreover, it can be observed that the intensity of all the absorption bands is enhanced for the colloids in comparison to the salt, effect which might be related to the low solubility of the BSS salt.

The calibration curve (mass-concentration in mg/L vs. maximum values of the absorption peak at 280–295 nm) described in “[Synthesis and characterization of the BSS nanoparticles](#)” section is shown in Fig. 5; the five samples used for the calibration are



**Fig. 5** Calibration curve obtained from the maximum values of the absorption peak at 280–295 nm versus the mass-concentration in mg/L for the samples deposited at different ablation times. The *blue circles* correspond to the samples used for the antimicrobial tests

shown as red squares. It can be observed that a good linear correlation ( $R^2 = 0.987$ ) was obtained, allowing the estimation of an equation to correlate absorption intensity with the BSS concentration. Figure 5 also shows that the absorption intensity of the BSS-20, BSS-30, BSS-45, and BSS-60 samples, shown as blue open circles, lies correctly in the correlation line. Therefore, the concentrations (mg/L) of these four samples were obtained using the equation shown in Fig. 5 and are included in Table 1.

The stability in time of the colloids is shown in Fig. 6. The absorption spectrum of a sample is shown as a function of the storage time. Most probably after 6 days the nanoparticles start to agglomerate since non-surfactant agents were used, so the absorption spectra were modified. Then all the characterization and the antibacterial experiments were done within this time window.

It is important to mention that the X-ray diffraction (XRD) patterns of the desiccated samples were also measured to obtain corroboration of the BSS structure. Figure 7 shows the pattern of one of the desiccated samples in comparison to the XRD pattern from original salt. The intensities have been normalized to the main peak for comparison, since the amount of material from the colloidal samples was much less; the intensity of their peaks was considerable smaller. Nevertheless, most of the BSS peaks were found in

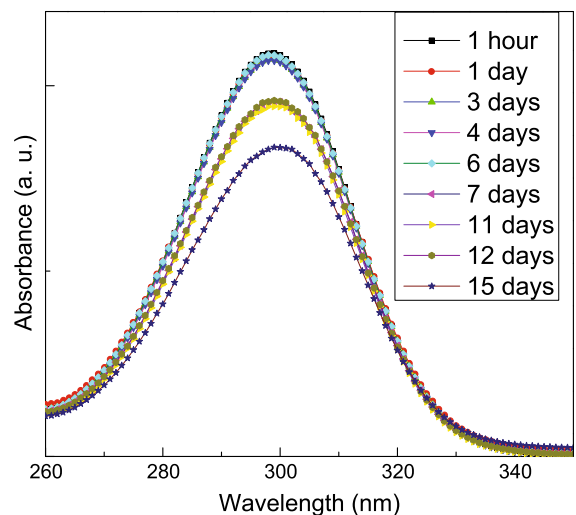


**Fig. 6** Amplification of the absorption spectra in the 260–340 nm in order to show the stability of the nanoparticles as a function of the storage time

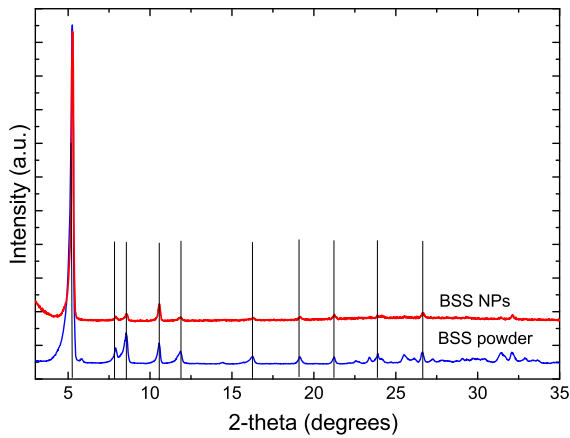


**Fig. 7** XRD of the powder obtained for the calibration curve was also characterized by X-ray diffraction and compared to the BSS original salt showing that similar patterns were obtained

both samples and they were in good coincidence with some of the reported data for bismuth subsalicylates (PDF cards 7001563 and 7001555), although not a perfect match was found due to the chemical heterogeneity of the BSS structure.

### Antibacterial activity

For the antibacterial test, the four different BSS nanoparticles samples described in Table 1 were used. The antibacterial effect of the bismuth subsalicylate colloids against the different bacterial strains was expressed as the inhibition ratio and is shown in Fig. 8a–d.

Figure 8a shows the inhibition ratio against *E. coli* and it can be seen that high inhibition ratios can be obtained for the BSS-60, BSS-30, and BSS-20 samples reaching nearly 90 %. Significant differences were observed using the BSS-20 sample, which corresponds to the minimum particle size (22 nm) and larger concentration (193 mg/L) sample.

When *P. aeruginosa* was exposed to the different BSS-NPs, the results showed that this strain was sensitive to all the BSS-NPs samples (Fig. 8b). An increasing inhibition ratio was observed as the particle size was decreased. Once again, sample BSS-20 was the most effective showing an inhibition ratio of 83 %. Significant differences were only observed between samples BSS-20 vs. BSS-45 and BSS-30 ( $P < 0.05$ ).

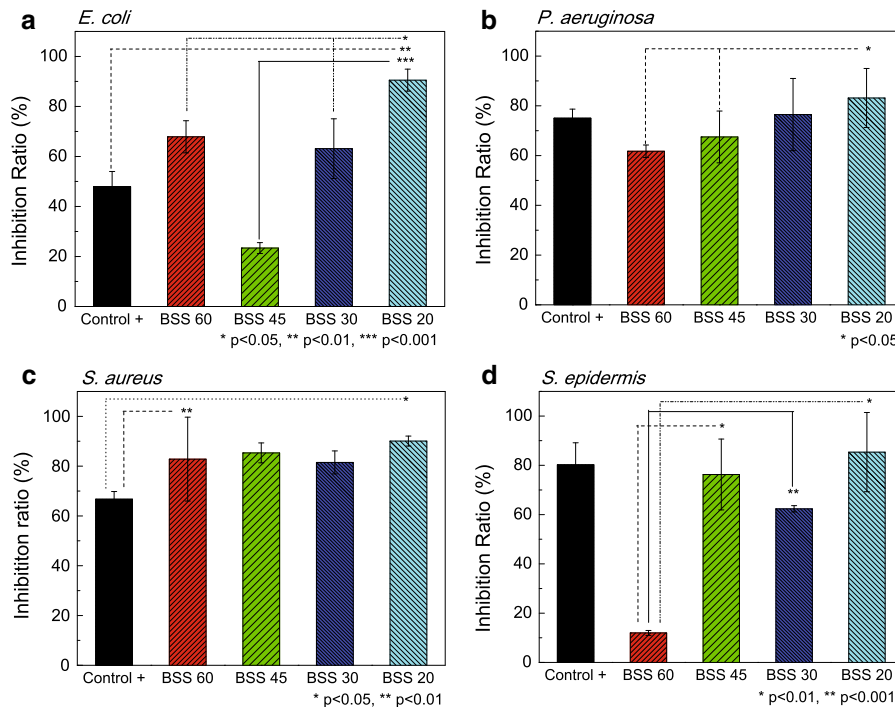


**Fig. 8** a, d Antibacterial effect (inhibition ratio) of the bismuth subsalicylate nanoparticles against a *E. coli*, b *P. aeruginosa*, c *S. aureus* and d *S. epidermidis*. The significances were estimated using the ANOVA test and Bonferronis modification

Similar findings were observed when *S. aureus* was tested, since all the samples showed a higher inhibition ratio than the antibiotic (Fig. 8c). Significant differences were found between BSS-20 versus positive control and BSS-30 versus positive control ( $P < 0.05$  and  $P < 0.01$ , respectively).

Finally, when *S. epidermidis* was tested (Fig. 8d), samples BSS-45, BSS-30, and BSS-20 presented a good antibacterial effect (76.2, 62.3, and 85.3 %, respectively), while sample BSS-60 shows an inhibition ratio of only 11.9 %, significantly lower than the other samples ( $P < 0.01$ ).

In general, it was observed that the inhibition ratio obtained for *E. coli* and *S. epidermidis* was affected by the NPs sizes and/or concentrations, meanwhile *P. aeruginosa* and *S. aureus* presented high bacterial-growth inhibition ratios independently of both the NP size and the concentration.

An additional experiment was carried out to elucidate the bactericidal (killing effect) or the bacteriostatic effect (inhibition of the growth) of the BSS nanoparticles. The bacterial growth of the four strains with and without BSS-20 NPs was measured during 4, 8, 12, 24, 36, 48, and 72 h. Bacterial growth curves are presented in Fig. 9. The results suggested that the BSS nanoparticles had a bactericidal effect on the four strains tested, since the logarithmic growth phase observed when bacteria were incubated only with the culture media was not attained when the BSS nanoparticles were added.

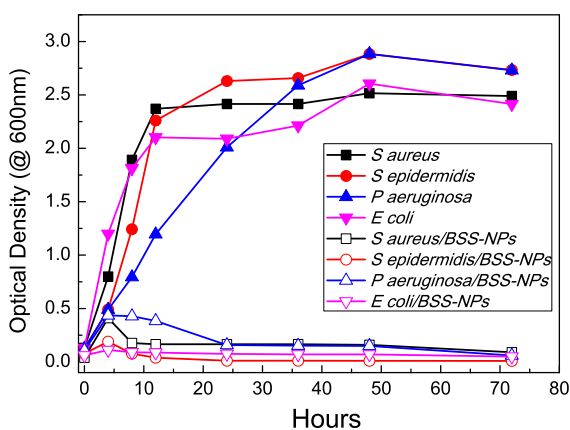


**Fig. 9** Bacterial growth curves of the four strains, with and without bismuth subsalicylate nanoparticles. The tests were performed using the BSS-20 sample

## Discussion

The laser ablation of solids immersed in liquids technique was employed in the present work in order to obtain nanoparticles of BSS in distilled water. This technique allows obtaining the colloids with different average sizes and concentrations by changing two parameters, the energy density (fluence) deposited on the target and the ablation time. In the present experiment, the output energy of the laser was kept constant, so that the fluence was varied by changing the size of the irradiated area on the target (spot size), which was done by changing the distance between the focusing lens and the target. A larger spot size produces a lower fluence and the results showed a trend indicating that the lower the fluence, the lower the nanoparticles size. This could be due to a lower mobility of the produced particles leading to a lower interaction between them, avoiding in this way the agglomeration that can induce an increase of the nanoparticle size. The concentration of the nanoparticles in a certain range of values can be varied by varying the ablation time, up to the moment when the liquid became highly saturated and the laser could not reach the target surface. This technique permits obtaining high purity BSS nanoparticles as no other chemical substances are needed for their production and the obtained colloids could be directly used in the antimicrobial tests, against four important opportunistic pathogens such as *E. coli*, *P. aeruginosa*, *S. aureus* and *S. epidermidis*. The structural and molecular characterization of the colloids demonstrated that bismuth subsalicylate nanoparticles were produced. The results showed similar or better antimicrobial effect than the antibiotic used as control (ciprofloxacin) on three of the four strains tested.

It is well known that the bactericidal effect of bismuth subsalicylate salts is limited due to their low solubility (Slikkerveer and de Wolff 1989), and it has been reported that at least 1–50 mM of BSS are required to inhibit the growth of species like *E. coli*, *Salmonella*, *Shigella* and *Campylobacter* sp. (Manhart 1990). In our study, the highest concentration tested was 193 mg/L (BSS-20 sample) equivalent to 0.533 mM, demonstrating the therapeutic potential use of antibacterial nanomaterials. Despite the fact that there are no published data regarding the synthesis and antimicrobial properties of BSS nanoparticles, some studies have reported the antibacterial and



antifungal effectiveness of zero-valent and bismuth oxide nanoparticles (Hernandez-Delgado et al. 2012, 2013) as well as the use of X-ray excited Bi nanoparticles to kill multidrug-resistant *P. aeruginosa* (Luo et al. 2013) and more recently, a paper reported the inhibition of *H. pylori* using carboxyl-capped bismuth nanoparticles (Nazari et al. 2014).

Since no other studies regarding the bactericidal effect of Bismuth subsalicylate nanoparticles were found, the following discussion presents a comparison between our results and the effect of other nanoparticles tested as antimicrobial agents for each one of the four strains tested, a summary of these studies is presented in Table 2.

With respect to *S. aureus*, we did not observed a strong dependence of the bacterial-growth inhibition ratio with either the concentration or the particle size, since all the BSS colloids were effective in killing the 80 % or more of the bacterial population. Tsuang et al. reported a 100 % inhibition of *S. aureus* using 20 nm TiO<sub>2</sub> UV activated nanoparticles; however to obtain this result a concentration of  $1 \times 10^3$  mg/L of TiO<sub>2</sub> nanoparticles was needed (Tsuang et al. 2008). In contrast, using the BSS-20 nanoparticles of similar average size (22 nm), we obtained a 90 % of growth inhibition with a concentration of 193 mg/L. Another study reported an inhibitory effect against *S. aureus* using 40 nm silver nanoparticles and a concentration of 80 mg/L (Fayaz et al. 2010) which are similar to the BSS-30, where we obtained an 81 % of growth inhibition using 95 mg/L. Lower concentration has only been reported to be effective when much smaller NPs are used, such as in the case of palladium nanoparticles reported by Adams et al. (Adams et al. 2014). In that paper, a concentration of 1.06 mg/L of Pd NPs was effective to attain 85 % of inhibition using 2.5 nm particles, 60 % using 2 nm, and 45 % using 3.1 nm particle size.

Regarding the inhibition of *P. aeruginosa*, the BSS nanoparticles with a particle size of 22 and a concentration of 193 mg/L showed the best antibacterial effect with an inhibition ratio of 83 %. Comparable results were reported using Bi nanoparticles of 30 nm and a concentration of 200 mg/L (92 % inhibition ratio) (Luo et al. 2013), as well as 100 % inhibition ratio (minimum inhibitory concentration, MIC) using ZnO nanoparticles with an average size of 13 nm and 220 mg/L (Feris et al. 2010). Other studies using silver nanoparticles have reported an 80 % and a

95 % of inhibition of *P. aeruginosa* (Khan et al. 2011; Morones et al. 2005), using particles of 43 nm and 10 nm at lower concentrations of 15 and 75 mg/L, respectively. Using TiO<sub>2</sub> UV-activated nanoparticles, a 100 % of inhibition (MIC:  $1 \times 10^3$  mg/L) of *P. aeruginosa* has been reported, although to achieve this result a high concentration and UV illumination were required (Tsuang et al. 2008).

The results obtained when *E. coli* and *S. epidermidis* were exposed to the BSS nanoparticles suggested that these strains were more sensitive to the nanoparticle size. For example, a 90 % inhibition of the growth of *E. coli* was obtained when the BSS-20 were used, while only a 23 % inhibition was obtained when the BSS-45 were tested. Different studies have reported a good antibacterial effect against *E. coli* using Ag nanoparticles; one study reported an 80 % of inhibition using a concentration of 75 mg/L and a particle size of 10 nm (Morones et al. 2005) and more interestingly, MIC concentrations of 30 mg/L were reported when using 40 nm silver nanoparticles (Fayaz et al. 2010). The antimicrobial effect of oxide nanoparticles has also been reported; Jiang et al. compared the effect of Al<sub>2</sub>O<sub>3</sub> (235 nm) and SiO<sub>2</sub> (46 nm) nanoparticles, reporting a 47 and 60 % of growth inhibition using a concentration of 20 mg/L (Jiang et al. 2009). Nanoparticles of NiO (25 nm), ZnO (40 nm) and CuO (79 nm) have showed bacterial inhibition ratios of 88, 71, and 77 %, respectively, against *E. coli* using a 20 mg/L concentration (Wang et al. 2010). Using Pd nanoparticles, a complete inhibition of the growth of *E. coli* was achieved using a concentration of 1.06 mg/L and a particle size of 2 nm; however, for larger Pd nanoparticles (2.5 and 3.1 nm) the inhibition of the growth decreases to the 70 % (Adams et al. 2014). These results indicated a size-dependent inhibition; lower sizes were more effective to inhibit the growth of *E. coli*. The effect of the concentration or the chemical composition is not so clear, meaning that studies about the antibacterial mechanism of action of the nanoparticles are required.

In the case of *S. epidermidis*, we observed that the nanoparticles with the higher particle size (BSS-60) and a concentration of 183 mg/L were the less effective, with only a 12 % of inhibition ratio, while the BSS-20 (193 mg/L) inhibited up to 85 % of the growth. Recently, the antibacterial effect of silver nanoparticles against *S. epidermidis* was reported; Tomita et al. reported a 90 % of inhibition using Ag-

**Table 2** Nanoparticle studies with antibacterial effect

Composition	Size (nm)	Concentration (mg/L)	Bacterial strain	Reference
Ag	43	From 1 to 30	<i>P. aeruginosa</i> , <i>B. subtilis</i> , and <i>K. pneumoniae</i>	Khan et al. (2011)
Ag	10	From 25 to 100	<i>P. aeruginosa</i> , <i>V. cholera</i> , <i>E. coli</i> and <i>S. typhus</i>	Morones et al. (2005)
Ag	40	80	<i>S. typhi</i> , <i>E. coli</i> , <i>S. aureus</i> and <i>M. luteus</i>	Fayaz et al. (2010)
Ag	1.5 to 40	From 1 to 5	<i>S. epidermidis</i> , <i>P. aeruginosa</i> , <i>E. coli</i> , <i>C. albicans</i> and <i>A. niger</i>	Bera et al. (2014)
Ag	16.65	From 15 to 30	<i>E. coli</i> , <i>P. aeruginosa</i> , <i>S. epidermidis</i> , <i>S. marcescens</i> and <i>E. faecalis</i>	Tomita et al. (2014)
Bi	3	104 and 418	<i>S. mutans</i>	Hernandez-Delgado et al. (2012)
Bi	30	2, 20 and 200	<i>P. aeruginosa</i>	Luo et al. (2013)
Bi <sub>2</sub> O <sub>3</sub>	77	From 116.5 to 932	<i>C. albicans</i>	Hernandez-Delgado et al. (2013)
CaO	16	112, 224 and 448	<i>P. aeruginosa</i> , <i>S. epidermidis</i> , and <i>C. tropicalis</i>	Roy et al. (2013)
Carboxyl-Capped Bi	100	From 40 to 140	<i>H. pylori</i>	Nazari et al. (2014)
Cu	25	312.5	<i>E. coli</i>	Rispoli et al. (2010)
NiO, ZnO, Fe <sub>2</sub> O <sub>3</sub> , Co <sub>3</sub> O <sub>4</sub> , CuO, TiO <sub>2</sub>	25, 40, 45, 69, 79, 33	20 and 100	<i>E. coli</i>	Wang et al. (2010)
Pd	2 to 3.1	From 0.00106 to 26.5	<i>E. coli</i> and <i>S. aureus</i>	Adams et al. (2014)
TiO <sub>2</sub>	20	10,000	<i>E. coli</i> , <i>P. aeruginosa</i> , <i>S. aureus</i> , <i>E. hirae</i> , and <i>B. fragilis</i>	Tsuang et al. (2008)
TiO <sub>2</sub> and ZnO	50	0.05 and 0.1	<i>S. epidermidis</i> and <i>S. aureus</i>	Lipovsky et al. (2011)
ZnO	13	From 79 to 325	<i>P. aeruginosa</i>	Feris et al. (2010)
ZnO	249	From 100 to 250	<i>E. coli</i>	Zhang et al. (2007)
ZnO	5 to 15.8	203 and 1,017	<i>K. pneumoniae</i> , <i>E. coli</i> , and <i>S. epidermidis</i>	Elmi et al. (2014)
ZnO	15 to 38	From 25 to 200	<i>K. pneumoniae</i> , <i>B. subtilis</i> , <i>E. aerogenes</i> , <i>S. epidermidis</i> , <i>C. albicans</i> and <i>M. pachydermatis</i>	Palanikumar et al. (2014)

tryptophane nanoparticles of 17 nm and a concentration of 20 mg/L (Tomita et al. 2014) and Bera et al. reported a MIC of 1.95 mg/L with fluorescent Ag nanoparticles of 1.5 nm (Bera et al. 2014). Finally, another study has reported the use of CaO nanoparticles to inhibit *S. epidermidis*, using a particle size of 16 nm and a MIC of 112 mg/L, and a minimum bactericidal concentration of 224 mg/L (Roy et al. 2013).

Collectively, our results suggest that a better bactericidal effect was always obtained with the smaller BSS-NPs. However, the effect of the concentration needs to be properly investigated, and further work is required in order to understand the antibacterial mechanism of action of the bismuth subsalicylate nanoparticles.

## Conclusions

The laser ablation of solids immersed in liquid media is an easy method that allowed synthesizing BSS nanoparticles with average sizes between 20 and 60 nm dispersed in distilled water. The size dispersion was relatively high, so it might not be suitable for production of monodispersed NPs, unless a size-selecting process is applied after deposition. Nevertheless, the tested colloids were efficient to inhibit bacterial growth of four pathogen strains in superior ratios than the antibiotic control, being the most efficient the BSS colloid with the minimum particle size (BSS-20).

These results suggest that BSS-NPs could be very interesting antibacterial agents with many applications in the medical area.

**Acknowledgements** The authors thank María de Jesús Salinas Nájera and Hermilo Zarco for their technical assistance. Supported by DGAPA-PAPIIT #IN18814, #IN118914, and CONACYT 152995 grants.

## References

- Adams CP, Walker KA, Obare SO, Docherty KM (2014) Size-dependent antimicrobial effects of novel palladium nanoparticles. PLoS ONE 9:e85981. doi:10.1371/journal.pone.0085981
- Alipour M, Dorval C, Suntres ZE, Omri A (2011) Bismuth-ethanedithiol incorporated in a liposome-loaded tobramycin formulation modulates the alginate levels in mucoid *Pseudomonas aeruginosa*. J Pharm Pharmacol 63:999–1007. doi:10.1111/j.2042-7158.2011.01304.x
- Andreasen JJ, Andersen LP (1987) In vitro susceptibility of *Campylobacter pyloridis* to cimetidine, sucralfate, bismuth and sixteen antibiotics. Acta Pathologica, Microbiologica, et Immunologica Scandinavica Sect B 95:147–149
- Andrews PC, Deacon GB, Forsyth CM, Junk PC, Kumar I, Maguire M (2006) Towards a structural understanding of the anti-ulcer and anti-gastritis drug bismuth subsalicylate. Angew Chem 45:5638–5642. doi:10.1002/anie.200600469
- Bera RK, Mandal SM, Raj CR (2014) Antimicrobial activity of fluorescent Ag nanoparticles. Lett Appl Microbiol 58:520–526. doi:10.1111/lam.12222
- Botequim D, Maia J, Lino MM, Lopes LM, Simoes PN, Ilharco LM, Ferreira L (2012) Nanoparticles and surfaces presenting antifungal, antibacterial and antiviral properties. Langmuir 28:7646–7656. doi:10.1021/la300948n
- Brogan AP, Verghese J, Widger WR, Kohn H (2005) Bismuth-dithiol inhibition of the *Escherichia coli* rho transcription termination factor. J Inorg Biochem 99:841–851. doi:10.1016/j.jinorgbio.2004.12.019
- Cornick NA, Silva M, Gorbach SL (1990) In vitro antibacterial activity of bismuth subsalicylate. Rev Infect Dis 12(Suppl 1):S9–S10
- Cremet L et al (2015) Pathogenic potential of *Escherichia coli* clinical strains from orthopedic implant infections towards human osteoblastic cells. Pathog Dis. doi:10.1093/femspd/ftv065
- Delchier JC, Malfertheiner P, Thieroff-Ekerdt R (2014) Use of a combination formulation of bismuth, metronidazole and tetracycline with omeprazole as a rescue therapy for eradication of *Helicobacter pylori*. Aliment Pharmacol Therap 40:171–177. doi:10.1111/apt.12808
- dos Santos CA et al (2014) Silver nanoparticles: therapeutic uses, toxicity, and safety issues. J Pharma Sci 103:1931–1944. doi:10.1002/jps.24001
- DuPont HL (1987) Bismuth subsalicylate in the treatment and prevention of diarrheal disease. Drug Intell Clin Pharm 21:687–693
- DuPont HL, Sullivan P, Pickering LK, Haynes G, Ackerman PB (1977) Symptomatic treatment of diarrhea with bismuth subsalicylate among students attending a Mexican university. Gastroenterology 73:715–718
- Elmi F et al (2014) The use of antibacterial activity of ZnO nanoparticles in the treatment of municipal wastewater. Water Sci Technol 70:763–770. doi:10.2166/wst.2014.232
- Ericsson CD, Evans DG, DuPont HL, Evans DJ Jr, Pickering LK (1977) Bismuth subsalicylate inhibits activity of crude toxins of *Escherichia coli* and *Vibrio cholerae*. J Infect Dis 136:693–696
- Fayaz AM, Balaji K, Girilal M, Yadav R, Kalaichelvan PT, Venketesan R (2010) Biogenic synthesis of silver nanoparticles and their synergistic effect with antibiotics: a study against gram-positive and Gram-negative bacteria. Nanomed-Nanotechnol 6:103–109
- Feris K et al (2010) Electrostatic interactions affect nanoparticle-mediated toxicity to Gram-negative bacterium *Pseudomonas aeruginosa* PAO1. Langmuir 26:4429–4436
- Ge R, Chen Z, Zhou Q (2012) The actions of bismuth in the treatment of *Helicobacter pylori* infections: an update. Metallomics 4:239–243. doi:10.1039/c2mt00180b

- Goodman CM, McCusker CD, Yilmaz T, Rotello VM (2004) Toxicity of gold nanoparticles functionalized with cationic and anionic side chains. *Bioconjugate Chem* 15:897–900. doi:[10.1021/bc049951i](https://doi.org/10.1021/bc049951i)
- Hajipour MJ et al (2012) Antibacterial properties of nanoparticles. *Trends Biotechnol* 30:499–511. doi:[10.1016/j.tibtech.2012.06.004](https://doi.org/10.1016/j.tibtech.2012.06.004)
- Harris LG, Foster SJ, Richards RG (2002) An introduction to *Staphylococcus aureus*, and techniques for identifying and quantifying *S. aureus* adhesins in relation to adhesion to biomaterials: review. *Eur Cell Mater* 4:39–60
- Hernandez L, Vazquez B, Lopez-Bravo A, Parra J, Goni I, Gurruchaga M (2007) Acrylic bone cements with bismuth salicylate: behavior in simulated physiological conditions. *J Biomed Mater Res, Part A* 80:321–332. doi:[10.1002/jbm.a.30947](https://doi.org/10.1002/jbm.a.30947)
- Hernandez-Delgadillo R, Velasco-Arias D, Diaz D, Arevalo-Nino K, Garza-Enriquez M, De la Garza-Ramos MA, Cabral-Romero C (2012) Zerovalent bismuth nanoparticles inhibit *Streptococcus mutans* growth and formation of biofilm. *Int J Nanomed* 7:2109–2113. doi:[10.2147/IJN.S29854](https://doi.org/10.2147/IJN.S29854)
- Hernandez-Delgadillo R, Velasco-Arias D, Martinez-Sanmiguel JJ, Diaz D, Zumeta-Dube I, Arevalo-Nino K, Cabral-Romero C (2013) Bismuth oxide aqueous colloidal nanoparticles inhibit *Candida albicans* growth and biofilm formation. *Int J Nanomed* 8:1645–1652. doi:[10.2147/IJN.S38708](https://doi.org/10.2147/IJN.S38708)
- Huh AJ, Kwon YJ (2011) “Nanoantibiotics”: a new paradigm for treating infectious diseases using nanomaterials in the antibiotics resistant era. *J Control Release* 156:128–145. doi:[10.1016/j.jconrel.2011.07.002](https://doi.org/10.1016/j.jconrel.2011.07.002)
- Jiang W, Mashayekhi H, Xing BS (2009) Bacterial toxicity comparison between nano- and micro-scaled oxide particles. *Environ Pollut* 157:1619–1625
- Khan SS, Mukherjee A, Chandrasekaran N (2011) Studies on interaction of colloidal silver nanoparticles (SNPs) with five different bacterial species. *Colloid Surf B* 87:129–138
- Kim EC, Lee BC, Chang HS, Lee W, Hong CU, Min KS (2008) Evaluation of the radiopacity and cytotoxicity of Portland cements containing bismuth oxide. *Oral Surg Oral Med Oral Pathol Oral Radiol Endod* 105:e54–e57. doi:[10.1016/j.tripleo.2007.08.001](https://doi.org/10.1016/j.tripleo.2007.08.001)
- Kim SH, Tramontina VA, Papalexou V, Lucyszyn SM, De Lima AA, do Prado AM (2012) Bismuth subgallate as a topical haemostatic agent at the palatal wounds: a histologic study in dogs. *Int J Oral Maxillofac Surg* 41:239–243. doi:[10.1016/j.ijom.2011.12.002](https://doi.org/10.1016/j.ijom.2011.12.002)
- Lipovsky A, Gedanken A, Nitzan Y, Lubart R (2011) Enhanced inactivation of bacteria by metal-oxide nanoparticles combined with visible light irradiation. *Lasers Surg Med* 43:236–240. doi:[10.1002/lsm.21033](https://doi.org/10.1002/lsm.21033)
- Luo Y, Hossain M, Wang CM, Qiao Y, An JC, Ma LY, Su M (2013) Targeted nanoparticles for enhanced X-ray radiation killing of multidrug-resistant bacteria. *Nanoscale* 5:687–694
- Mahony DE, Woods A, Eelman MD, Burford N, Veldhuyzen van Zanten SJ (2005) Interaction of bismuth subsalicylate with fruit juices, ascorbic acid, and thiol-containing substrates to produce soluble bismuth products active against *Clostridium difficile*. *Antimicrob Agents Chemother* 49:431–433. doi:[10.1128/AAC.49.1.431-433.2005](https://doi.org/10.1128/AAC.49.1.431-433.2005)
- Manhart MD (1990) In vitro antimicrobial activity of bismuth subsalicylate and other bismuth salts. *Rev Infect Dis* 12(Suppl 1):S11–S15
- Markowska K, Grudniak AM, Wolska KI (2013) Silver nanoparticles as an alternative strategy against bacterial biofilms. *Acta Biochim Pol* 60:523–530
- Mijnendonckx K, Leys N, Mahillon J, Silver S, Vanhoudt R (2013) Antimicrobial silver: uses, toxicity and potential for resistance. *Biometals* 26:609–621. doi:[10.1007/s10534-013-9645-z](https://doi.org/10.1007/s10534-013-9645-z)
- Morones JR, Elechiguerra JL, Camacho A, Holt K, Kouri JB, Ramirez JT, Yacaman MJ (2005) The bactericidal effect of silver nanoparticles. *Nanotechnology* 16:2346–2353
- Nazari P et al (2014) The antimicrobial effects and metabolomic footprinting of carboxyl-capped bismuth nanoparticles against *Helicobacter pylori*. *Appl Biochem Biotechnol* 172:570–579. doi:[10.1007/s12010-013-0571-x](https://doi.org/10.1007/s12010-013-0571-x)
- Pacifico L, Osborn JF, Anania C, Vaira D, Olivero E, Chiesa C (2012) Review article: bismuth-based therapy for *Helicobacter pylori* eradication in children. *Aliment Pharmacol Ther*. doi:[10.1111/j.1365-2036.2012.05055.x](https://doi.org/10.1111/j.1365-2036.2012.05055.x)
- Palanikumar L, Ramasamy SN, Balachandran C (2014) Size-dependent antimicrobial response of zinc oxide nanoparticles. *IET Nanobiotechnol* 8:111–117. doi:[10.1049/iet-nbt.2012.0008](https://doi.org/10.1049/iet-nbt.2012.0008)
- Pardo OA, Pardo Castello V (1952) The treatment of early syphilis with penicillin and bismuth subsalicylate; follow-up report. *Am J Syph Gonorrhoea Vener Dis* 36:342–345
- Purvis JE (1926) CV.: the absorption spectra of various derivatives of salicylic acid. *J Chem Soc* 48:775–778
- Purvis JE (1927) The absorption spectra of various alkaloids and their salicylates and of derivatives of salicylic acid. *J Chem Soc*:2715–2719
- Riool M et al (2014) *Staphylococcus epidermidis* originating from titanium implants infects surrounding tissue and immune cells. *Acta Biomater* 10:5202–5212. doi:[10.1016/j.actbio.2014.08.012](https://doi.org/10.1016/j.actbio.2014.08.012)
- Rispoli F, Angelov A, Badia D, Kumar A, Seal S, Shah V (2010) Understanding the toxicity of aggregated zero valent copper nanoparticles against *Escherichia coli*. *J Hazard Mater* 180:212–216. doi:[10.1016/j.jhazmat.2010.04.016](https://doi.org/10.1016/j.jhazmat.2010.04.016)
- Roy A, Gauri SS, Bhattacharya M, Bhattacharya J (2013) Antimicrobial activity of CaO nanoparticles. *J Biomed Nanotechnol* 9:1570–1578
- Rybtke M, Hultqvist LD, Givskov M, Tolker-Nielsen T (2015) *Pseudomonas aeruginosa* biofilm infections: community structure, antimicrobial tolerance and immune response. *J Mol Biol*. doi:[10.1016/j.jmb.2015.08.016](https://doi.org/10.1016/j.jmb.2015.08.016)
- Schaller M, Laude J, Bodewaldt H, Hamm G, Korting HC (2004) Toxicity and antimicrobial activity of a hydrocolloid dressing containing silver particles in an ex vivo model of cutaneous infection. *Skin Pharmacol Physiol* 17:31–36. doi:[10.1159/000074060](https://doi.org/10.1159/000074060)
- Serena T et al (2007) Bismuth subgallate/borneol (suile) is superior to bacitracin in the human forearm biopsy model for acute wound healing. *Adv Skin Wound Care* 20:485–492. doi:[10.1097/01.ASW.0000288208.85807.b8](https://doi.org/10.1097/01.ASW.0000288208.85807.b8)
- Shaikh AR, Giridhar R, Yadav MR (2007) Bismuth-norfloracin complex: synthesis, physicochemical and antimicrobial

- evaluation. *Int J Pharm* 332:24–30. doi:[10.1016/j.ijpharm.2006.11.037](https://doi.org/10.1016/j.ijpharm.2006.11.037)
- Slikkerveer A, de Wolff FA (1989) Pharmacokinetics and toxicity of bismuth compounds. *Med Toxicol Advers Drug Exp* 4:303–323
- Sox TE, Olson CA (1989) Binding and killing of bacteria by bismuth subsalicylate. *Antimicrob Agents Chemother* 33:2075–2082
- Steinhoff MC, Douglas RG Jr, Greenberg HB, Callahan DR (1980) Bismuth subsalicylate therapy of viral gastroenteritis. *Gastroenterology* 78:1495–1499
- Tillman LA, Drake FM, Dixon JS, Wood JR (1996) Review article: safety of bismuth in the treatment of gastrointestinal diseases. *Aliment Pharmacol Therap* 10:459–467
- Tomita RJ, de Matos RA, Vallim MA, Courrol LC (2014) A simple and effective method to synthesize fluorescent nanoparticles using tryptophan and light and their lethal effect against bacteria. *J Photochem Photobiol, B* 140C:157–162. doi:[10.1016/j.jphotobiol.2014.07.015](https://doi.org/10.1016/j.jphotobiol.2014.07.015)
- Tramontina VA, Machado MA, Nogueira Filho Gda R, Kim SH, Vizzioli MR, Toledo S (2002) Effect of bismuth subgallate (local hemostatic agent) on wound healing in rats. *Histol Histometric Find Braz Dent J* 13:11–16
- Tsuang YH, Sun JS, Huang YC, Lu CH, Chang WHS, Wang CC (2008) Studies of photokilling of bacteria using titanium dioxide nanoparticles. *Artif Organs* 32:167–174
- Wang ZP, Lee YH, Wu B, Horst A, Kang YS, Tang YJJ, Chen DR (2010) Anti-microbial activities of aerosolized transition metal oxide nanoparticles. *Chemosphere* 80:525–529
- Weir E, Lawlor A, Whelan A, Regan F (2008) The use of nanoparticles in anti-microbial materials and their characterization. *Analyst* 133:835–845. doi:[10.1039/b715532h](https://doi.org/10.1039/b715532h)
- Yang G (2012) *Laser ablation in liquids: principles and applications in the preparation of nanomaterials*. Pan Stanford Publishing Pte Ltd, Boston
- Zhang LL, Jiang YH, Ding YL, Povey M, York D (2007) Investigation into the antibacterial behaviour of suspensions of ZnO nanoparticles (ZnO nanofluids). *J Nanopart Res* 9:479–489